Alteration of the Iron–Sulfur Cluster Composition of *Escherichia coli* Dimethyl Sulfoxide Reductase by Site-Directed Mutagenesis†

Richard A. Rothery and Joel H. Weiner*

Department of Biochemistry, 474 Medical Sciences Building, University of Alberta, Edmonton, Alberta, Canada T6G 2H7

Received March 18, 1991; Revised Manuscript Received June 10, 1991

ABSTRACT: We have used site-directed mutagenesis to alter the [Fe–S] cluster composition of *Escherichia coli* dimethyl sulfoxide (DMSO) reductase (DmsABC). The electron-transfer subunit (DmsB) of this enzyme contains 16 Cys residues arranged in 4 groups (I–IV) which provide ligands to 4 [4Fe–4S] clusters [Cammack, R., & Weiner, J. H. (1990) *Biochemistry 29*, 8410–8416]. Strong homologies exist between these Cys groups and the four Cys groups of the electron-transfer subunit (NarH) of *E. coli* nitrate reductase (NarGHJI), which contains a [3Fe–4S] cluster in addition to multiple [4Fe–4S] clusters. The Cys group primarily involved in providing ligands to the [3Fe–4S] cluster of NarH has a Trp residue at a position equivalent to Cys_{102} of DmsB. We have mutated Cys_{102} to Trp, Ser, Tyr, and Phe and have investigated the altered enzymes in terms of their enzymatic activities and EPR properties. The mutant enzymes do not support electron transfer from menaquinol to DMSO, although they retain high rates of electron transport from reduced benzyl viologen to DMSO. The mutations cause major changes in the EPR properties of the enzyme in the fully reduced and oxidized states. In the oxidized state, new species are observed in all the mutants; these have spectral features comprising a peak at $g = 2.03$ (g_z) and a peak–trough at $g = 2.00$ (g_{xy}). The temperature dependencies, microwave power dependencies, and spin quantitations of these species are consistent with the Trp_{102}, Ser_{102}, Phe_{102}, and Tyr_{102} mutations causing conversion of one of the [4Fe–4S] clusters present in the wild-type enzyme into [3Fe–4S] clusters in the mutant enzymes.

Escherichia coli, when grown anaerobically with dimethyl sulfoxide (DMSO)[1] as respiratory oxidant, develops a respiratory chain terminated by a membrane-bound menaquinol:DMSO oxidoreductase (DMSO reductase; Bilous & Weiner, 1985a,b; Sambasivarao et al., 1990). The operon encoding DMSO reductase (*dmsABC*) has been cloned (Bilous & Weiner, 1988) and sequenced (Bilous et al., 1988), and the enzyme it encodes has been purified to homogeneity (Weiner et al., 1988). DMSO reductase is a complex iron–sulfur molybdoenzyme consisting of a molybdopterin-containing catalytic subunit (DmsA, 87.4 kDa), an [Fe–S] cluster containing electron-transfer subunit (DmsB, 23.1 kDa), and a membrane anchor subunit (DmsC, 30.8 kDa). Cells harboring the cloned *dmsABC* operon express large quantities of active DMSO reductase (Bilous & Weiner, 1988), making this enzyme readily amenable to studies involving genetic manipulations and site-directed mutagenesis of the cloned operon.

The EPR properties of the purified and in situ enzyme have recently been reported (Cammack & Weiner, 1990). DmsB appears to contain four [4Fe–4S] clusters, and this results in the observation of a complex EPR spectrum in the fully reduced state which has features similar to spectra of other proteins containing multiple [4Fe–4S] clusters, such as *Clostridium pasteurianum* ferredoxin (Prince & Adams, 1987) and *Micrococcus lactilyticus* ferredoxin (Mathews et al., 1974). Ligands to the 4 [4Fe–4S] clusters of DmsB are thought to be provided by the 16 Cys residues present in this subunit. These residues are arranged in four groups (I–IV; Cammack & Weiner, 1990), and these have sequences similar to the Cys groups ligating the [4Fe–4S] clusters of many bacterial ferredoxins (Bilous et al., 1988; Bruschi & Guerlesquin, 1988). The [Fe–S] clusters in DmsB have midpoint potentials ($E_{m,7}$) of −50, −120, −240, and −330 mV (Cammack & Weiner, 1990), but it is not known which Cys groups ligate the clusters corresponding to the reported midpoint potentials.

Significant homologies exist between the catalytic and electron-transfer subunits of DMSO reductase and *E. coli* nitrate reductase (NarGHJI; Blasco et al., 1989). The electron-transfer subunit of nitrate reductase (NarH) also contains 4 groups of Cys residues in a similar arrangement to that found in DmsB, although in this case there are 15 rather than 16 such residues present in the 4 groups. NarH also contains two additional Cys residues outside of the ferredoxin-type sequence groups (Blasco et al., 1989). The difference in Cys group composition between NarH and DmsB is located in the group of Cys residues in NarH corresponding to group III of DmsB. A Trp is found at the position equivalent to Cys_{102} of DmsB. Significantly, EPR and MCD characterizations of nitrate reductase indicate that this enzyme contains a [3Fe–4S] center in addition to multiple [4Fe–4S] clusters (Johnson et al., 1985a). The sequence of the minor nitrate reductase of *E. coli*, NarZYWV, has recently been determined (Blasco et al., 1990). This enzyme also has an electron-transfer subunit (NarY) containing four groups of Cys residues, and as is the case in NarH, the Cys group corresponding to group III of DmsB has a Trp residue at the position in the sequence equivalent to Cys_{102} of DmsB. It would therefore be interesting to mutagenize Cys_{102} of DmsB to determine if the [Fe–S] cluster composition of DMSO reductase can be made similar to that reported for nitrate reductase (NarGHJI) by Johnson et al. (1985a).

† This work was funded by a grant from the Medical Research Council of Canada to J.H.W. (MT5838). R.A.R. is a Postdoctoral Fellow of the Alberta Heritage Foundation for Medical Research.

* Author to whom correspondence should be addressed.

[1] Abbreviations: BV, benzyl viologen; DMSO, dimethyl sulfoxide; EPR, electron paramagnetic resonance; MCD, magnetic circular dichroism; TMAO, trimethylamine *N*-oxide.

0006-2960/91/0430-8296$02.50/0

Table I: Bacterial Strains and Plasmids

strain or plasmid	description	source
E. coli strains		
HB101	*supE*44 *hsdS*20 (r_B-m_B-) *recA*13 *ara*-14 *proA*2 *lacY*1 *galK*2 *rpsL*20 *xyl*-5 *mtl*-1	lab collection
TG1	*supE hsd*Δ5 *thi* Δ(*lac-proAB*) *F'* [*traD36 proAB*$^+$ *lacI*^{q} *lacZ*ΔM15]	Amersham
JM101	*supE thi* Δ(*lac-proAB*) *F'* [*traD36 proAB*$^+$ *lacI*^{q} *lacZ*Δ'15]	L. Fliegel[a]
DSS301	TG1, Δ*dmsABC*	lab collection[b]
plasmids		
pTZ18R	Amp^R*lacZ'*	Pharmacia
pBR322	Tet^{R}Amp^R	Pharmacia
pDMS160	pBR322 Amp^R (*dmsABC*)$^+$	this study
pDMS222	pTZ18R Amp^R (*dmsABC*)$^+$	Bilous & Weiner (1988)
pDMS223	pTZ18R Amp^R (*dmsABC*)$^+$	this study
pDMS160-C102F	pBR322 Amp^R (*dmsAB*[$C_{102} \rightarrow F_{102}$]*C*)$^+$	this study
pDMS160-C102S	pBR322 Amp^R (*dmsAB*[$C_{102} \rightarrow S_{102}$]*C*)$^+$	this study
pDMS160-C102W	pBR322 Amp^R (*dmsAB*[$C_{102} \rightarrow W_{102}$]*C*)$^+$	this study
pDMS160-C102Y	pBR322 Amp^R (*dmsAB*[$C_{102} \rightarrow Y_{102}$]*C*)$^+$	this study
phage		
M13K07	Kan^R	Pharmacia

[a] Department of Biochemistry, University of Alberta. [b] D. Samasivarao and J. H. Weiner, unpublished results.

In this paper, we have used the combined techniques of oligonucleotide-directed mutagenesis and electron paramagnetic resonance spectroscopy to study the effect of amino acid substitutions of Cys_{102} on the [Fe–S] cluster composition of *E. coli* DMSO reductase.

Materials and Methods

Bacterial Strains and Plasmids. The *E. coli* strains and plasmids used in this study are listed in Table I. Strain DSS301 (D. Sambasivarao and J. H. Weiner, unpublished results) is a derivative of strain TG1 which lacks the entire *dmsABC* operon. Routine cloning work was carried out with strain TG1, studies of the expression of mutant and wild-type enzyme were carried out with strains DSS301 and HB101, and EPR characterizations were carried out primarily with strain HB101. All manipulations of plasmids and strains were carried out essentially as described by Sambrook et al. (1989).

pDMS223 is a derivative of pDMS222 (pTZ18R vector, Pharmacia) which lacks a 1.66 kbp noncoding DNA fragment 3' to *dmsC* (Bilous & Weiner, 1988). It was constructed by introducing a new *Sal*I site into pDMS222 by oligonucleotide-directed mutagenesis (see below for mutagenesis protocol), followed by elimination of the 1.66 kbp fragment by *Sal*I digestion and ligation. pDMS160 was constructed by subcloning a 4.83 kbp *Eco*RI–*Sal*I fragment containing the cloned *dmsABC* operon from pDMS223 into pBR322 (Pharmacia).

Oligonucleotide-Directed Mutagenesis. Oligonucleotide-directed mutagenesis of Cys_{102} was carried out by using the Amersham in vitro mutagenesis system (Taylor et al., 1985). Oligonucleotides for mutagenesis and sequencing were synthesized by using Applied Biosystems 381A and 391 oligonucleotide synthesizers. The mutagenesis oligonucleotides differed from the published DNA sequence in the region of *dmsB* encoding Cys_{102} by having an appropriate nucleotide substitution or by having a mixture of nucleotides at an appropriate position. The mutagenesis reactions were performed by using single-stranded pDMS223 as template. Single-stranded template was prepared by superinfection of *E. coli* JM101/pDMS223 with helper phage M13K07 (Pharmacia) as described by Sambrook et al. (1989). Putative mutant progeny from the oligonucleotide-diected mutagenesis reactions were initially screened by plasmid miniprep and restriction endonuclease mapping. Only those progeny having restriction maps identical with that of pDMS223 were selected for further screening by dideoxy sequencing (Sequenase Version 2.0 DNA sequencing kit, United States Biochemical Corp.). Because the presence of the *dmsABC* operon cloned into the high copy number vector pTZ18R results in inhibition of anaerobic growth of the host strain on minimal media (P. T. Bilous and J. H. Weiner, unpublished results), the mutagenized *dmsABC* operons were subcloned by *Eco*RI/*Sal*I digestion into an *Eco*RI/*Sal*I digest of the moderate copy number vector pBR322. The presence of the mutations in the pBR322-based plasmids was confirmed by dideoxy sequencing.

Growth of Bacteria. For initial biochemical analysis, the mutant plasmids were transformed into DSS301 (Δ*dmsABC*). Cells were grown anaerobically at 37 °C on a glycerol–DMSO minimal medium (Bilous & Weiner, 1985a), glycerol–fumarate minimal medium, or glucose–peptone–fumarate rich medium as described previously (Condon & Weiner, 1988). Growth on glycerol–fumarate medium was for 24 h (DSS301 strains) or 48 h (HB101 strains) in 20-L batch cultures. Growth on rich medium was for 18 h in 250-mL batches. For phage and plasmid manipulations and for preparation of inocula for batch cultures, cells were grown aerobically on Luria–Bertani medium (Sambrook et al., 1989) or Terrific broth (Tartof & Hobbs, 1987). Where appropriate, ampicillin (100 μg mL^{-1}), streptomycin (100 μg mL^{-1}), and kanamycin (50 μg mL^{-1}) were included in the growth media.

Cell Harvesting and Isolation of Cytoplasmic Membranes. Cells were harvested and membranes prepared by French pressure cell lysis and differential centrifugation as described by Cammack and Weiner (1990). We have found that under some circumstances the presence of either TMAO or DMSO in preparations containing DMSO reductase serves to stabilize the enzyme activity (D. Sambasivarao and J. H. Weiner, unpublished results); therefore, the buffer used for washing cells contained 50 mM MOPS (pH 7.0), 70 mM TMAO, and 5 mM EDTA. Prior to cell lysis, the serine protease inhibitor phenylmethanesulfonyl fluoride was added to a final concentration of 0.2 mM. Cytoplasmic membranes (in 50 mM MOPS, 70 mM TMAO, and 5 mM EDTA, pH 7.0) were frozen by pipetting dropwise into liquid nitrogen and were then stored at −70 °C. Prior to use, the membranes were thawed and diluted in 100 mM MOPS (pH 7.0) containing 5 mM EDTA and then pelleted by high-speed centrifugation before being resuspended in this buffer at a protein concentration of around 30 mg mL^{-1}.

Enzyme Assays. DMSO- and TMAO-dependent oxidation of reduced benzyl viologen (BV) was determined as previously described (Cammack & Weiner, 1990). Fumarate-dependent oxidation of reduced BV was determined as described by Bilous and Weiner (1985a). Nitrate-dependent oxidation of reduced BV was measured by using the same protocol as for

Table II: Growth Characteristics of Cells Harboring Mutant and Wild-Type DMSO Reductase Plasmids

plasmid	doubling time (h) in *E. coli* DSS301	doubling time (h) in *E. coli* HB101
pBR322	NG[a]	7.7[b]
pDMS160	4.09	3.4
pDMS160-C102W	NG	15.5
pDMS160-C102S	NG	19.4
pDMS160-C102F	NG	10.7
pDMS160-C102Y	NG	13.8

[a] Abbreviation: NG, no growth on glycerol–DMSO minimal medium. [b] Doubling times were determined from measurements of cell densities in glycerol–DMSO minimal medium using a Klett–Summerson spectrophotometer equipped with a no. 66 filter.

DMSO/TMAO-dependent oxidation, but with 35 mM potassium nitrate as substrate.

EPR Spectroscopy. Samples for EPR spectroscopy were prepared as described by Cammack and Weiner (1990). Unless otherwise stated, samples were of membranes prepared from cells grown anaerobically on glycerol–fumarate minimal medium. Spectra were recorded by using a Bruker ESP300 EPR spectrometer equipped with an Oxford Instruments ESR-9 flowing helium cryostat. Instrument conditions and temperatures are described in the individual figure legends, and spectra were corrected for tube calibrations. Spin quantitations were carried out by truncated double integrations with base-line corrections as described by Cammack and Weiner (1990). Microwave power saturation data were plotted and fitted to an empirical equation as described by Rupp et al. (1978).

Results

Preparation of Oligonucleotide-Directed Mutants of Cys_{102} in DmsB. We have changed Cys_{102} of DmsB to Trp, Ser, Tyr, and Phe by introducing single nucleotide base substitutions into pDMS223 (Table I). These mutations were verified by dideoxy sequencing, and no mutations other than those specified by the mutagenesis oligonucleotides were detected. The mutagenized operons were subcloned into pBR322, and expression of the mutant enzymes was verified by polyacrylamide gel electrophoresis and immunoblot analysis using the anti-DmsA and anti-DmsB immunoglobulins isolated by Sambasivarao et al. (1990). These analyses confirm that large quantities of enzyme are expressed from the mutant plasmids and that the mutant enzymes are associated with the cytoplasmic membrane fraction of lysed cells (data not shown).

Growth Properties and Enzymatic Activities of the Cys_{102} Mutants. The ability of the Cys_{102} mutants to support respiratory growth on a glycerol–DMSO minimal medium was studied by using the Δ*dmsABC* strain DSS301 (Table I; D. Sambasivarao and J. H. Weiner, unpublished results). This strain can only support growth on glycerol–DMSO when it is transformed with a plasmid bearing the *dmsABC* operon such as pDMS160. The effect of expression of large amounts of plasmid-encoded mutant enzyme on the growth on glycerol–DMSO medium of cells possessing a wild-type chromosomal *dmsABC* operon was investigated by using HB101. Table II summarizes the results of these growth experiments. All of the substitutions of Cys_{102} result in loss of growth on glycerol–DMSO in DSS301 transformed with the mutant plasmids, indicating that the mutations block electron flow from menaquinol to DMSO. When HB101 transformed with the mutant plasmids is grown on glycerol–DMSO, there is significant inhibition of growth compared to the control strain HB101/pBR322. This result is consistent with normal assembly of mutant enzymes into the cytoplasmic membrane resulting in competition between chromosomally encoded (wild type) and plasmid-encoded (mutant) DmsB subunits. Such effects have been previously reported in studies of mutants of fumarate reductase (Weiner et al., 1986; Westenberg et al., 1990).

Table III: Enzyme Activities of Membranes Containing Amplified Levels of Mutant and Wild-Type DMSO Reductase[a]

strain	specific activity[b] DMSO	TMAO	fumarate	nitrate
DSS301/pBR322	ND[c]	ND	7.0	0.24
DSS301/pDMS160	8.5	69.1	3.4	0.18
DSS301/pDMS160-C102W	8.1	60.5	6.1	0.20
DSS301/pDMS160-C102S	9.7	85.2	4.9	0.36
HB101/pBR322	0.92	8.8	4.5	0.39
HB101/pDMS160	10.4	92.9	3.3	0.45
HB101/pDMS160-C102W	17.8	172.8	3.3	1.3
HB101/pDMS160-C102S	15.4	147.9	2.6	0.63
HB101/pDMS160-C102F	17.8	162.1	2.9	0.99
HB101/pDMS160-C102Y	10.8	117.4	2.8	0.99

[a] Membranes were prepared from glycerol–fumarate-grown cells as described under Materials and Methods and were suspended in 100 mM MOPS (pH 7) containing 5 mM EDTA. [b] Enzyme activities are expressed as BV:substrate (DMSO, TMAO, fumarate, or nitrate) oxidoreductase activities in units of micromoles of benzyl viologen oxidized per milligram of membrane protein per minute. Assays were carried out at 23 °C. The data are representative of two experiments. [c] ND, not detected.

To minimize potential artifacts due to chromosomally encoded wild-type DMSO reductase, we initially attempted to characterize the mutants of Cys_{102} in membrane preparations from DSS301 grown on a glycerol–fumarate minimal medium. Table III shows the DMSO, TMAO, fumarate, and nitrate reductase activities of membranes using the artifical electron donor reduced benzyl viologen (BV). DMSO and TMAO are alternative substrates for DMSO reductase (Weiner et al., 1988), and we measured the nitrate reductase activities of our membranes to explore the possibility that one or more of our mutant enzymes may catalyze nitrate reduction. Expression of the plasmid-encoded mutant and wild-type enzymes results in amplification of BV:DMSO oxidoreductase activity in both DSS301 and HB101. EPR spectra of membranes from DSS301/pBR322 indicate that this strain contains amplified levels of fumarate reductase centers FR1 and FR3 compared to HB101/pBR322 (see below). When we compared the BV:fumarate oxidoreductase activities of DSS301/pBR322 and HB101/pBR322 membranes, we found higher levels of activity in the DSS301 strain (specific activities of 7.0 and 4.5, respectively). With the exception of DSS301/pDMS160, all of the DSS301 strains have amplified BV:fumarate activities compared to the equivalent HB101 strains (Table III). As the fumarate reductase signals interfere with analysis of mutant and wild-type DMSO reductase EPR spectra, we decided to carry out the bulk of the EPR studies reported herein on membranes prepared from HB101. EPR studies with DSS301 are reported as they provide a unique opportunity to study the functional activity of the wild-type and mutant DMSO reductases (see below).

Table III also shows the BV:nitrate reductase activities of the mutant enzymes in *E. coli* HB101 and DSS301 membranes. Although the $Cys_{102} \rightarrow Trp_{102}$ substitution results in apparent minor amplification of the BV:nitrate activity in HB101, no amplification is observed in DSS301.

In choosing *E. coli* HB101 to characterize the mutants of DMSO reductase in situ using EPR spectroscopy, the effect of the nonmutant chromosomally encoded enzyme has to be considered. Expression of the enzyme from pDMS160 results in an approximate 10-fold amplification of enzymic activity

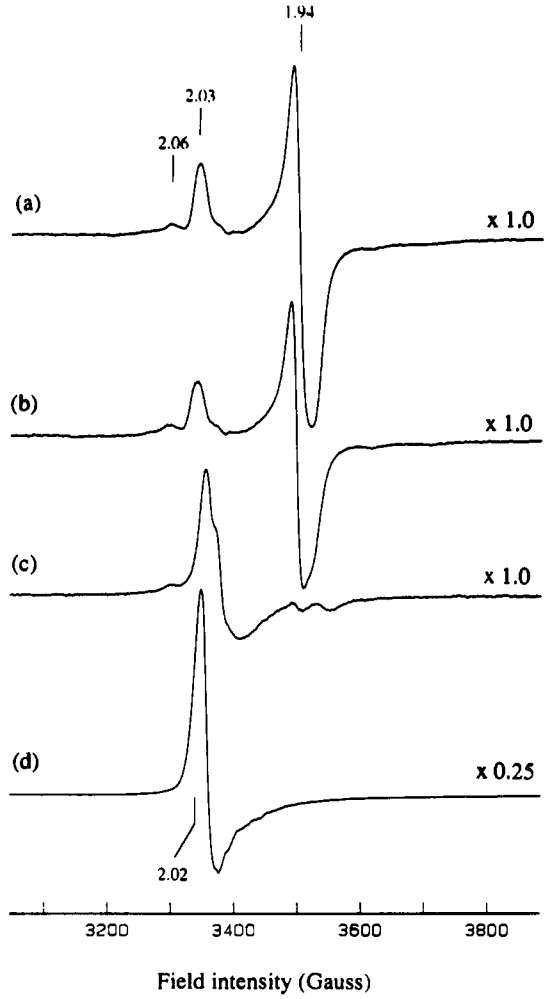

FIGURE 1: EPR spectra of DSS301/pBR322 membranes. The spectra are of membranes from glycerol–fumarate-grown DSS301/pBR322: (a) dithionite reduced (5 mM); (b) dithionite reduced (5 mM) and treated with 25 mM DSMO; (c) dithionite reduced (5 mM) and treated with 25 mM fumarate; (d) air oxidized. Dithionite-reduced membranes were incubated under argon for 1 min at 23 °C prior to being frozen. Following addition of DMSO or fumarate, samples were incubated for a further minute. Air-oxidized samples were vigorously stirred for 45 s with a coiled stainless-steel wire prior to being frozen. Spectra were recorded under the following conditions: temperature, 12 K; microwave power, 20 mW; microwave frequency, 9.48 GHz; modulation amplitude, 10 G_{pp} at 100 kHz; gain, 2×10^4. Spectra were corrected for protein concentration to a nominal 30 mg mL^{-1}.

compared to expression from the chromosome alone (as in HB101/pBR322). While this appears to indicate that 90% of the enzyme arises from the plasmid, it is not consistent with the data indicating that complementation of the wild-type chromosomal copy of the operon with the mutant plasmids causes inhibition of glycerol on glycerol–DMSO. The doubling times of HB101 harboring the mutant plasmids are increased by factors of between 1.4 (HB101/pDMS160-C102F) and 2.5 (HB101/pDMS160-C102S) compared to the control HB101/pBR322 (Table II). These observations suggest that >90% of the enzymatic activity in HB101 transformed with the mutant plasmids arises from the plasmids rather than from the chromosome.

EPR Characterization of DSS301 Membranes. Figure 1 shows EPR spectra at 12 K of membranes from DSS301/pBR322, showing the effects of dithionite reduction followed by addition of DMSO and fumarate. Noticeable in the dithionite-reduced spectrum (Figure 1a) are a major peak at $g = 2.03$ and a peak–trough at around $g = 1.94$. These features are characteristic of the g_z and g_{xy} of the reduced [2Fe–2S] cluster, FR1, of fumarate reductase (Johnson et al., 1988; Cammack et al., 1986). Addition of 25 mM DMSO (Figure 1b) or TMAO (not shown) has little effect on the intensities of the FR1 g_z and g_{xy}. Addition of fumarate results in diminution of the FR1 spectral features and the appearance of a near-isotropic signal with a sharp peak at $g = 2.02$ with a broader trough immediately upfield (Figure 1c). These features are characteristic of the oxidized [3Fe–4S] center FR3 of fumarate reductase (Johnson et al., 1985b, 1988). These results confirm that the DSS301 membranes contain significant quantities of EPR-detectable fumarate reductase. The effect of DMSO and TMAO on the EPR spectrum of reduced DSS301/pBR322 membranes, when compared to their effect on the spectrum of reduced DSS301/pDMS160 membranes (see below), confirms the absence of menaquinol:DMSO oxidoreductase activity in DSS301/pBR322 membranes.

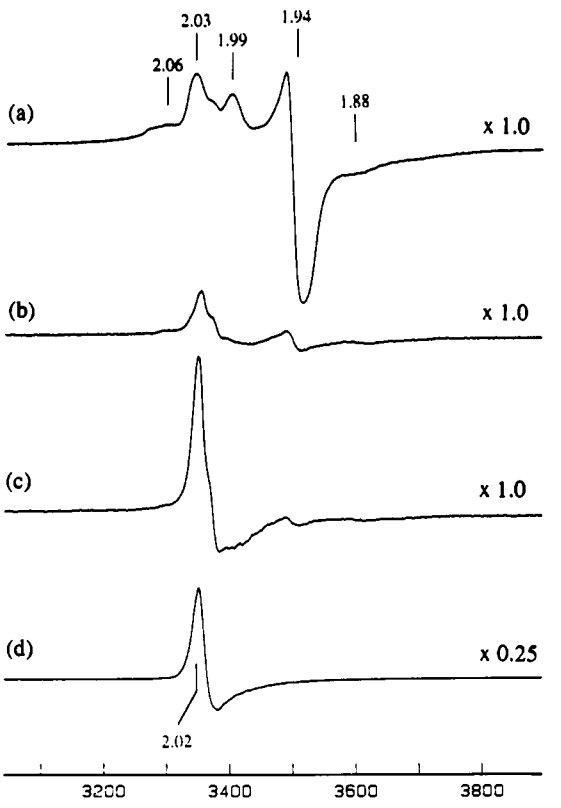

FIGURE 2: EPR spectra of DSS301/pDMS160 membranes. The spectra are of membranes from glycerol–fumarate-grown DSS301/pDMS160: (a) dithionite reduced (5 mM); (b) dithionite reduced (5 mM) and treated with 25 mM DSMO; (c) dithionite reduced (5 mM) and treated with 25 mM fumarate; (d) air oxidized. Sample preparations, protein concentrations, and EPR conditions were as described for Figure 1.

Figure 2 shows EPR spectra at 12 K of membranes from DSS301/pDMS160, showing the effects of dithionite reduction followed by addition of DMSO and fumarate. The spectrum of dithionite-reduced DSS301/pDMS160 membranes (Figure 2a) contains the features of the fumarate reductase center FR1 described above. In addition, a broad spectrum of lower intensity is observed in the background. This spectrum has features resolvable from those of FR1 comprising a broad shoulder at $g = 2.06$, a peak at $g = 1.99$, and a trough at $g = 1.88$. The spectrum reported for dithionite-reduced DMSO reductase by Cammack and Weiner (1990) includes the non-FR1 features present in Figure 2a. Addition of 25 mM DMSO (Figure 2b), TMAO (not shown), or fumarate (Figure 2c) results in diminution of all the features of the di-

thionite-reduced DSS301/pDMS160 spectrum and the appearance of the FR3 signal described above. Significantly, addition of fumarate abolishes the DMSO reductase spectral features, and addition of DMSO or TMAO abolishes the FR1 spectral features. These data indicate that DMSO or TMAO is able to oxidize fumarate reductase centers FR1 and FR3 via a functional DMSO reductase and the menaquinol pool. Likewise, fumarate is able to oxidize the [Fe–S] clusters of the wild-type DMSO reductase via the menaquinol pool.

When DSS301/pDMS160-C102W and DSS301/pDMS160-C102S membranes were studied as described above, it was found that the relative intensities of the FR1 signals compared to the DMSO reductase [Fe–S] signals are greater than is the case with DSS301/pDMS160 membranes. This made detection of the EPR signals of the mutant enzymes in DSS301 membranes difficult (data not shown). However, the effects of the substrates DMSO, TMAO, and fumarate on DSS301/pDMS160-C102W and DSS301/pDMS160-C102S membranes are as described above for DSS301/pBR322 membranes (Figure 1), indicating that these mutants of DMSO reductase are defective in electron transfer through DmsB to and from the menaquinol pool.

Because of the large overlapping EPR signals due to the [Fe–S] clusters of fumarate reductase and the lower BV: DMSO oxidoreductase activities of membranes from DSS301/pDMS160 compared to HB101/pDMS160 (see above), we decided to carry out further EPR characterizations of the mutant forms of DMSO reductase in membrane preparations from HB101.

EPR Characterization of Dithionite-Reduced HB101 Membranes Containing Amplified Levels of *Wild-Type and Mutant DMSO Reductase.* Figure 3 shows EPR spectra recorded at 12 K of dithionite-reduced membranes from HB101 transformed with pBR322, pDMS160, and the mutant plasmids. The spectrum of membranes from HB101/pBR322 (Figure 3a) contains sharp peaks at $g = 2.03$ and $g = 1.94$. These features are identical with the intense fumarate reductase FR1 signals observed in Figures 1 and 2. Minor broad background signals are also observed in reduced HB101/pBR322 membranes with features around $g = 2.06$ and $g = 1.88$.

The spectrum of dithionite-reduced membranes from HB101/pDMS160 (Figure 3b) is very similar to that reported for the membrane-bound and purified DMSO reductase by Cammack and Weiner (1990). Noticeable in the spectrum of HB101/pDMS160 membranes are peaks at $g = 2.06$, $g = 2.03$, $g = 1.99$, and $g = 1.95$. Troughs are observed at $g = 1.92$ and $g = 1.88$. Comparison of the spectrum of HB101/pDMS160 membranes with that of HB101/pBR322 membranes suggests that the peak at $g = 2.03$ arises from the g_z of fumarate reductase center FR1. The g_{xy} of FR1 is also likely to contribute to the $g = 1.95$ to $g = 1.92$ peak–trough of the EPR spectrum of DMSO reductase in HB101 membranes.

Figure 3c–f shows spectra of dithionite-reduced membranes containing the mutants of DMSO reductase. Clearly, the mutations of Cys_{102} of DMSO reductase have major effects on the EPR spectrum of the dithionite-reduced enzyme. The two most noticeable changes are a loss of the $g = 1.99$ peak and a deepening of the $g = 1.88$ trough. An additional minor shoulder/peak is also observed at $g = 1.94$, which along with the peaks observed at $g = 2.03$ can be assigned to the spectrum of FR1. Also, there is a significant broadening of the low-field side of the mutant spectra compared to the spectrum of HB101/pDMS160 membranes.

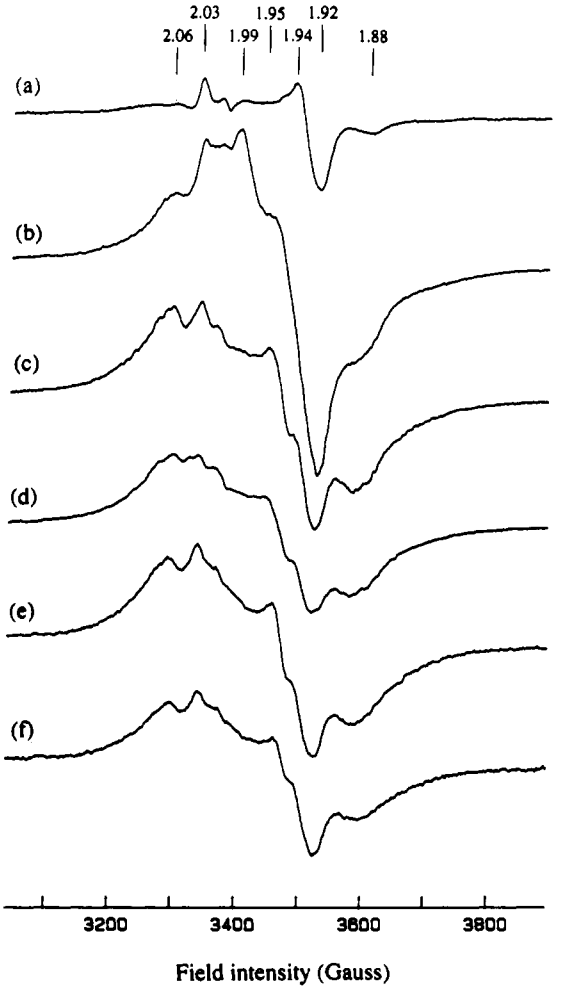

FIGURE 3: EPR spectra of dithionite-reduced membranes from HB101 containing wild-type and mutant forms of DMSO reductase. Samples (at 30 mg mL^{-1} protein) were reduced with 5 mM dithionite under argon for 2 min before being frozen. Spectra were recorded of (a) HB101/pBR322, (b) HB101/pDMS160, (c) HB101/pDMS160-C102W, (d) HB101/pDMS160-C102S, (e) HB101/pDMS160-C102F, and (f) HB101/pDMS160-C102Y. EPR instrument conditions and protein concentrations were as described for Figure 1.

While the spectrum of HB101/pDMS160 membranes can be interpreted in terms of the presence of two pairs of interacting [4Fe–4S] centers in the wild-type enzyme (Cammack & Weiner, 1990), the spectra of the Cys_{102} mutants are indicative of a more complex situation (see Discussion). The spectra of membranes containing the wild-type and mutant enzymes are well resolved at 12 K and 20 mW, and at higher temperatures (>30 K), the spectral features are almost broadened out. Power saturation studies (data not shown) indicate that the signals are all difficult to saturate within the available microwave power range (power for half-saturation, $P_{1/2} > 100$ mW at 12 K). Such behavior is consistent with the mutant and wild-type enzymes containing [4Fe–4S] clusters.

In order to establish that the changes elicited by the substitutions of Cys_{102} are not due to sensitization of the enzyme to oxidative damage during the protocol used to prepare the membranes used in this work, we decided to investigate the EPR properties of intact HB101 cells harboring pBR322, pDMS160, and the mutant plasmids. It is known that many [4Fe–4S] clusters of the bacterial ferredoxins are sensitive to oxidative damage; these include *Desulfovibrio africanus* ferredoxin III (George et al., 1989) and *Pyrococcus furiosus* ferredoxin (Conover et al., 1990). Figure 4 shows spectra of

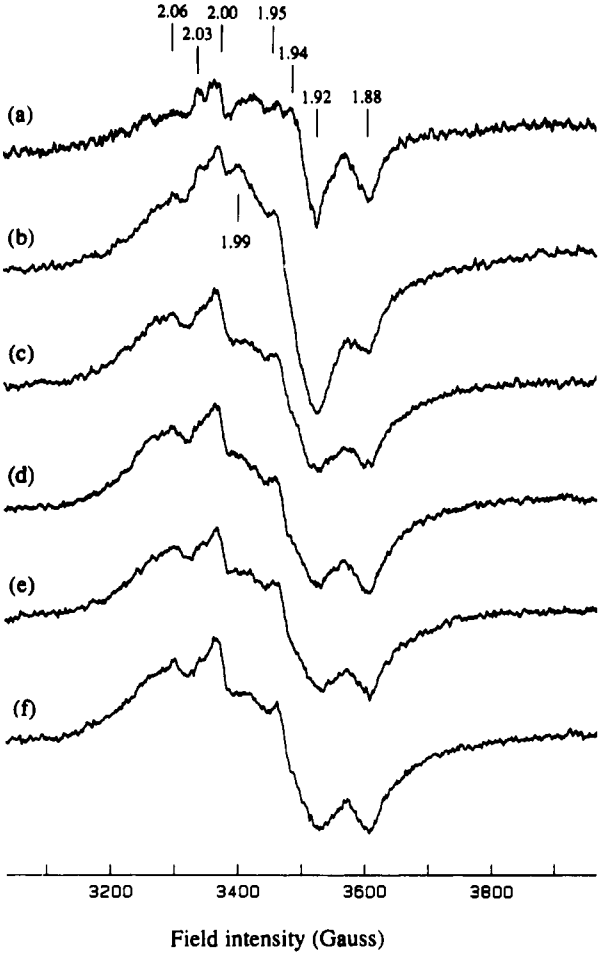

FIGURE 4: EPR spectra of dithionite-reduced whole cells from HB101 containing wild-type and mutant forms of DMSO reductase. Cells were grown for 18 h on a glucose–peptone–fumarate medium and were harvested and washed in degassed 100 mM MOPS (pH 7) containing 5 mM EDTA and 20 mM succinate. Cells were reduced with dithionite as described for Figure 1. Spectra were recorded of cells from (a) HB101/pBR322, (b) HB101/pDMS160, (c) HB101/pDMS160-C102W, (d) HB101/pDMS160-C102S, (e) HB101/pDMS160-C102F, and (f) HB101/pDMS160-C102Y. EPR instrument conditions and protein concentrations were as described for Figure 1.

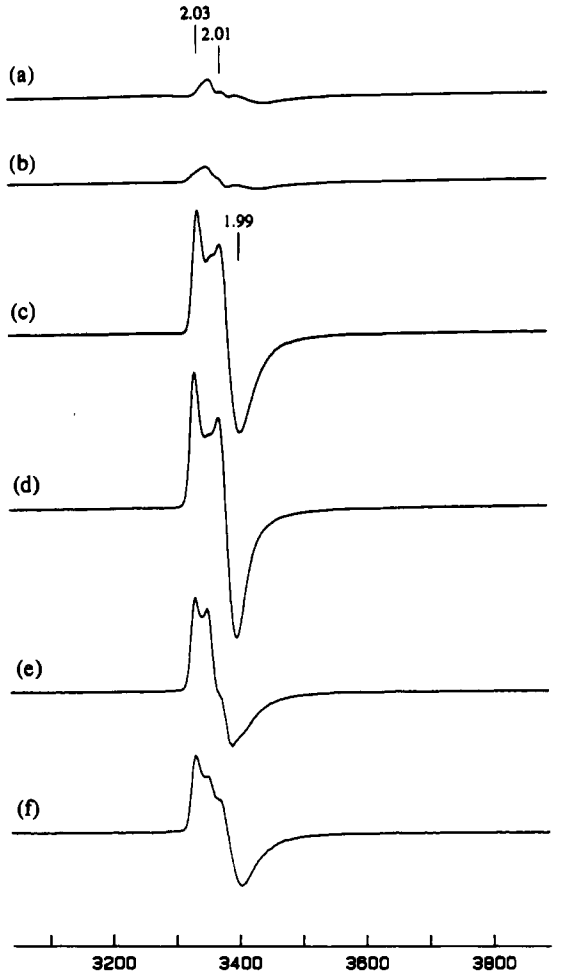

FIGURE 5: EPR spectra of ferricyanide-oxidized membranes from HB101 containing wild-type and mutant forms of DMSO reductase. Samples (at 30 mg mL^{-1} protein) were oxidized with 140 μM ferricyanide for 2 min before being frozen. Spectra were recorded of (a) HB101/pBR322, (b) HB101/pDMS160, (c) HB101/pDMS160-C102W, (d) HB101/pDMS160-C102S, (e) HB101/pDMS160-C102F, and (f) HB101/pDMS160-C102Y. EPR instrument conditions and protein concentrations were as described for Figure 1, except that the gain was 5×10^3.

dithionite-reduced cells grown on a glucose–peptone–fumarate rich medium, harvested, and washed in nitrogen-saturated buffer containing 20 mM succinate as substrate to maintain anaerobiosis. Comparison of the spectrum of HB101/pBR322 cells with that of HB101/pDMS160 cells indicates that the bulk of the EPR-detectable [Fe–S] clusters in the latter are constituents of DMSO reductase. The spectra of cells containing the mutants of DMSO reductase are similar to the spectra shown in Figure 3. These data indicate that the EPR properties of the mutant DMSO reductases in intact cells are the same as they are in membrane preparations. Minor differences between the whole cell and membrane preparations are presumably due to the greater concentrations of non-DMSO reductase [Fe–S] clusters in the former, presumably due to the different growth medium and/or due to the presence of cytoplasmic [Fe–S] clusters.

EPR Characterization of Oxidized Membranes from HB101 Containing Amplified Levels of Wild-Type and Mutant DMSO Reductase. Figure 5 shows EPR spectra of ferricyanide-oxidized membranes from HB101 transformed with pBR322, pDMS160, and the mutant plasmids. HB101/pBR322 and HB101/pDMS160 membranes have essentially similar spectra, with a minor peak at $g = 2.02$ attributable to the [3Fe–4S] FR3 cluster of fumarate reductase. The FR3 signals detectable in membranes from HB101 are much less intense than those present in membranes from DSS301 (cf. Figures 5 and 1). The spectra of HB101 membranes containing the mutants of DMSO reductase contain major new features. The spectra of HB101/pDMS160-C102W (Figure 5c) and HB101/pDMS160-C102S (Figure 5d) membranes are very similar, with an intense peak at $g = 2.03$ and an intense peak–trough centered at $g = 2.00$. The spectra of HB101/pDMS160-C102F (Figure 5e) and HB101/pDMS160-C102Y (Figure 5f) membranes are similar to those of HB101/pDMS160-C102W and HB101/pDMS160-C102S membranes, but the ratios of the $g = 2.00$ peak–trough to the $g = 2.03$ peak are lower in these two spectra. In the spectrum of HB101/pDMS160-C102F, there is more structure in the center of the spectrum constituting a peak at $g = 2.02$. Membrane samples oxidized with the alternative oxidant dichlorophenolindophenol (1.1 mM final concentration) exhibit spectra identical with those of Figure 5. The EPR-detectable centers responsible for the spectra of the mutant enzymes can be attributed to centers having axial symmetry with approximate g values of $g_z = 2.03$ and $g_{xy} =$

Table IV: Spin Quantitations of the [Fe–S] EPR Signals of Mutant and Wild-Type DMSO Reductase

plasmid	spin concentrations[a] [nmol (mg of protein)$^{-1}$]				ratios		
	DR[b]	AO	DO	FO	ENZ[c]	DR/DO	DR/FO
pBR322	0.36	0.05	0.08	0.05		4.50	7.20
pDMS160	1.79	0.07	0.05	0.11	0.45	35.8	16.3
pDMS160-C102W	1.71	0.19	0.47	0.55	0.57	3.64	3.11
pDMS160-C102S	1.33	0.07	0.34	0.54	0.44	3.91	2.46
pDMS160-C102F	1.69	0.14	0.38	0.46	0.56	4.45	3.67
pDMS160-C102Y	1.18	0.22	0.36	0.40	0.39	3.27	2.95

[a] These were determined by double integration of spectra of samples recorded under nonsaturating conditions (12 K and 2 mW). The samples were prepared by addition of 5 mM dithionite, 1.1 mM dichlorophenolindophenol, or 140 μM ferricyanide. Air-oxidized samples were prepared by vigorously stirring the membrane samples in an EPR tube with a coiled stainless-wire. [b] Abbreviations: DR, dithionite reduced; AO, air oxidized; DO, dye (dichlorohenolindohenol) oxidized; ENZ, enzyme; FO, ferricyanide oxidized. [c] Enzyme concentrations (in nanomoles per milligram of protein) were estimated from the dithionite-reduced spin quantitations assuming that the wild-type enzyme has four spins per molecule and that the mutants each have three spins per molecule. No attempt was made to correct for the presence of contaminating non-DMSO reductase signals.

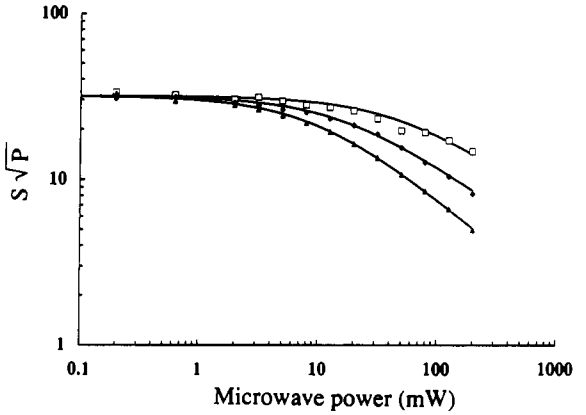

FIGURE 6: Power dependence of the oxidized species present in the mutants of DMSO reductase. The saturation behavior of the g = 2.03 peak of the oxidized species is plotted and fitted to the empirical equation of Rupp et al. (1978). Data were obtained from spectra recorded at 10 K. Membranes were from DSS301/pBR322 (□), HB101/pDMS160-C102W (♦), and HB101/pDMS160-C102S (▲). Data were fitted to $P_{1/2}$'s of 50 mW (DSS301/pBR322), 16 mW (HB101/pDMS160-C102W), and 10 mW (HB101/pDMS160-C102S).

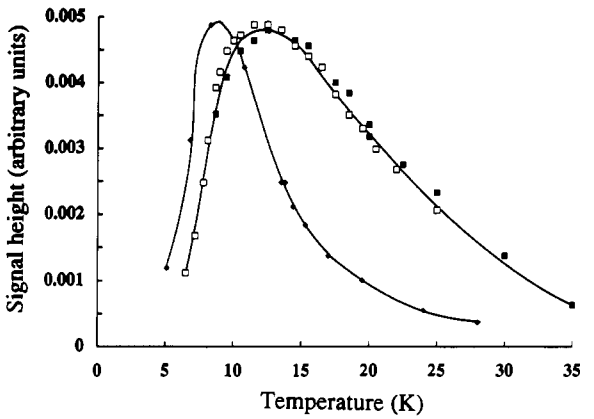

FIGURE 7: Temperature dependence of the oxidized species present in the mutants of DMSO reductase. The intensities of the FR3 g = 2.02 peak and the mutant g = 2.03 peaks are plotted versus temperature. Spectra were recorded by using a microwave power of 20 mW and are normalized to a maximum intensity. Membranes were from DSS301/pBR322 (♦), HB101/pDMS160-C102W (□), and HB101/pDMS160-C102S (■).

2.00. We have assigned the new EPR signals observed in oxidized membranes containing the mutant DMSO reductases to oxidized [3Fe–4S] clusters (see Discussion).

A minor anomaly exists between the intensities of the features of the reduced and oxidized spectra of HB101/pDMS160-C102S compared to the spectra of the other mutants. The intensities of the features of the reduced spectrum are lower than those of the spectra of the other mutants, whereas the intensities of the features of the oxidized spectrum are higher than those of the spectra of the other mutants. This anomaly may be due to variations in the spin–spin interactions between the [Fe–S] clusters of the reduced enzyme and the extent of formation of the species visible in the oxidized enzyme between the different mutants.

Figure 6 shows the power dependence of the new signals of oxidized HB101/pDMS160-C102W and HB101/pDMS160-C102S membrane samples at 10 K. Also included is the power dependence of the [3Fe–4S] signal attributed to center FR3 in DSS301/pBR322 membranes. While the g = 2.02 peak of the FR3 signal of fumarate reductase has a $P_{1/2}$ of 50 mW, the $P_{1/2}$ values of the signals of the mutants of DMSO reductase are 16, 10, and 2 mW for the $C_{102} \rightarrow W_{102}$, $C_{102} \rightarrow S_{102}$, and $C_{102} \rightarrow F_{102}$ mutants, respectively. The $P_{1/2}$ of the oxidized signal of the $C_{102} \rightarrow Y_{102}$ mutant is difficult to estimate, due to the presence of multiple components in the saturation curve (of approximately 2 and 50 mW, data not shown), indicating a heterogeneity of protein conformations in this case.

Figure 7 shows the effect of temperature on the intensities of the signals of the new species and on the FR3 signal of DSS301/pBR322 membranes. The FR3 signal present in DSS301/pBR322 membranes reaches peak intensity (at 20 mW) at around 8 K, and decreases rapidly with increasing temperature until at around 30 K it is barely visible. The signals of the new species present in oxidized membranes containing the $C_{102} \rightarrow W_{102}$ and $C_{102} \rightarrow S_{102}$ mutants reach peak intensity at around 13 K, and are still visible at 30 K. The $C_{102} \rightarrow F_{102}$ and $C_{102} \rightarrow Y_{102}$ mutants of the enzyme exhibit similar temperature behavior to the Trp and Ser mutants.

Quantitations of the New EPR-Visible Species Present in HB101 Membranes Containing the Mutant Forms of DMSO Reductase. Table IV summarizes the results of quantitations of the EPR-visible species reported herein. Dithionite-reduced membranes from HB101/pDMS160 contain EPR-visible [Fe–S] clusters at a concentration of 1.79 nmol (mg of protein)$^{-1}$. This value is in close agreement with the value of 1.80 nmol (mg of protein)$^{-1}$ reported by Cammack and Weiner (1990) for DMSO reductase in membranes from HB101/pDMS159. The concentrations of [Fe–S] clusters in membranes containing amplified levels of the mutant enzymes are in the range 1.18–1.71 nmol (mg of protein)$^{-1}$. From the total EPR-detectable [Fe–S] cluster concentrations, it is possible to estimate the concentrations of the wild-type and mutant enzymes in HB101 membranes. Assuming that the mutant enzymes contain three [4Fe–4S] clusters and that the wild-type enzyme contains four such clusters, the specific enzyme con-

centrations can be estimated to be between 0.39 and 0.57 nmol (mg of protein)$^{-1}$ (Table IV).

Three strategies were used to attempt to oxidize the new species present in membranes overexpressing the mutant enzymes; these were air oxidation, dichlorophenolindophenol oxidation, and ferricyanide oxidation. The use of alternative oxidants was necessary, as ferricyanide is known to oxidatively degrade some [4Fe–4S] clusters to [3Fe–4S] clusters (Beinert & Thomson, 1983; Ohmori et al., 1986). Dichlorophenolindophenol was chosen as an alternative oxidant as it has a midpoint potential ($E_{m,7}$) of +217 mV, and it has often been used as an effective mediator in redox titrations (Wilson, 1978).

The quantitations of oxidized membranes in Table IV indicate that air oxidation is effective in oxidizing the [3Fe–4S] centers of HB101/pBR322 and HB101/pDMS160 membranes, but it does not appear to be sufficient to oxidize the new EPR-visible species in the mutant membranes. This indicates that the new species have relatively high midpoint potentials compared to the [3Fe–4S] clusters of fumarate reductase ($E_{m,7}$ = −70 mV; Cole et al., 1985) and nitrate reductase ($E_{m,7}$ = +80 mV; Vincent, 1979). To oxidize the new species, it is necessary to add 1.1 mM dichlorophenolindophenol or 140 μM ferricyanide. Ferricyanide-oxidized membranes containing the mutant forms of DMSO reductase contain EPR-detectable species in the concentration range 0.40–0.55 nmol (mg of protein)$^{-1}$. Interestingly, the ratios of dithionite-reduced EPR-visible species to ferricyanide-oxidized species fall in the range 2.46–3.67, with a mean of 3.05. Given the experimental error inherent in quantitations such as those reported herein and the presence of non-DMSO reductase EPR-detectable [Fe–S] clusters in the membranes (principally from fumarate reductase), the quantitations are consistent with the conversion of one of the EPR-detectable [4Fe–4S] clusters of the wild-type enzyme into a cluster visible in the oxidized state in each of the Cys_{102} mutants, viz., a [3Fe–4S] cluster.

Discussion

The results reported herein indicate the importance of the [4Fe–4S] cluster to which Cys_{102} of DmsB provides a ligand to the overall function of *E. coli* DMSO reductase in electron transfer from menaquinol to DMSO. None of the amino acid substitutions at this position results in an enzyme capable of supporting respiratory growth on glycerol–DMSO minimal medium, indicating that this [4Fe–4S] cluster is essential for efficient electron transfer from menaquinol to DMSO. However, all of the mutants have high BV:DMSO oxidoreductase activities, indicating that the pathway of electrons from BV to DMSO is distinct from that of electrons from menaquinol to DMSO. The quantitations of Table IV indicate that the concentrations of the mutant and wild-type DMSO reductases in membranes from HB101 are all approximately equal. On this basis, the amplified BV:DMSO and BV:TMAO reductase activities found for the mutant enzymes (Table III) indicate that the turnover numbers of the mutant enzymes with BV as reductant are higher than that of the wild-type enzyme.

The presence of intense fumarate reductase FR1 and FR3 signals in spectra of membranes from the *dmsABC* deletion strain DSS301 made this strain unsuitable for detailed EPR characterizations of the wild-type and mutant DMSO reductases reported herein. However, we have been able to use the presence of the fumarate reductase EPR signals to study electron transfer between DMSO reductase and the menaquinol pool. Centers FR1 and FR3 have midpoint potentials ($E_{m,7}$) of −20 and −70 mV (Cole et al., 1985), respectively, so both these centers should respond to the redox state of the menaquinol pool ($E_{m,7}$ = −74 mV; Ingledew & Poole, 1984). We used the FR1 and FR3 signals to show that the mutant enzymes do not exchange electrons with the menaquinol pool. It is likely that the FR1 and FR3 signals of a strain such as DSS301 (or other strains in which fumarate reductase is deliberately overexpressed from a plasmid) could be used to probe the menaquinol:substrate oxidoreductase activities of other respiratory chain enzymes.

The temperature and power dependencies of the EPR spectra of the dithionite-reduced mutant enzymes are consistent with the presence of EPR-visible [4Fe–4S] clusters, and in this respect, the mutants are similar to the wild type. However, the line shapes of the EPR signals of the dithionite-reduced mutants are all significantly different from that of the wild type. Because of the magnetic interactions between the clusters, it is not possible to assign the various features to individual clusters of the enzyme. However, we conclude that the loss of the g = 1.99 peak in the mutant spectra is due to conversion of one of the [4Fe–4S] clusters of the wild-type enzyme to a [3Fe–4S] cluster. We attribute the broadening of the mutant line shape on the low-field side of the spectrum to interactions between the S = 2 paramagnetic reduced [3Fe–4S] cluster (EPR invisible) and one or more of the reduced EPR-visible [4Fe–4S] clusters (EPR visible). Such interactions have been reported in bacterial 7Fe ferredoxins (Hagen et al., 1985). Spin quantitations of the EPR spectra of the mutant enzymes are consistent with the mutations causing conversion of the [4Fe–4S] cluster ligated primarily by Cys group III in the wild-type enzyme into [3Fe–4S] clusters in the mutant enzymes.

The oxidized spectra of the mutant enzymes in situ are qualitatively similar to those reported for the [3Fe–4S] clusters of the seven-iron ferredoxins of *Thermus thermophilus* (Ohnishi et al., 1980; Hagen et al., 1985) and *Thermodesulphobacterium commune* (Guigliarelli et al., 1986). They are distinct from the near-isotropic signals observed under similar conditions for the [3Fe–4S] clusters of *E. coli* nitrate reductase (Johnson et al., 1985a) and fumarate reductase (Johnson et al., 1985b). The power and temperature behavior of the mutant [3Fe–4S] signals are similar to those of the inactivated form of aconitase which contains a [3Fe–4S] cluster (Ohnishi et al., 1975). We have therefore assigned the new signals observed in oxidized membrane preparations containing the mutants of DMSO reductase to new [3Fe–4S] clusters. Further studies are in progress to corroborate this assignment using MCD spectroscopy.

A surprising result to come out of this work is that all the amino acid substitutions made for Cys_{102} of DysB result in the ligation of a new [3Fe–4S] cluster by the mutagenized Cys group III. Our initial expectation was that some of the mutants would completely lose the cluster ligated by the first three Cys residues of group III. To our knowledge, there are no natural [3Fe–4S] clusters which are ligated by Cys groups having Phe or Tyr residues at the position equivalent to Cys_{102}. The Cys group primarily involved in providing ligands to the S3 [3Fe–4S] cluster of *Bacillus subtilis* succinate dehydrogenase has a Ser residue at the position equivalent to Cys_{102} of DmsB (Phillips et al., 1987), and many other [3Fe–4S] clusters are ligated by sequences having Val or Ile at this position (George et al., 1985; Bruschi & Guerlesquin, 1988). Further studies are in progress to determine the effects of substituting Val and Ile for Cys_{102} and for other Cys residues in DmsB.

The failure of air oxidation to oxidize the new [3Fe–4S] clusters of the mutant enzymes indicates that their midpoint

DmsB	99	Cys	Ile	Gly	Cys	Arg	Tyr	Cys	His	Met	Ala	Cys	Pro
NarH	217	Cys	Arg	Gly	Trp	Arg	Met	Cys	Ile	Thr	Gly	Cys	Pro
NarY	216	Cys	Arg	Gly	Trp	Arg	Leu	Cys	Ile	Ser	Gly	Cys	Pro

potentials are much higher than those of the other redox-active components. Preliminary potentiometric analyses of the $C_{102} \rightarrow W_{102}$ mutant indicate that in this case the midpoint potential of the new cluster is >150 mV (R. A. Rothery and J. H. Weiner, unpublished results). The behavior of all of the mutant enzymes with respect to air oxidation can be explained if the [3Fe–4S] midpoint potentials are >150 mV, as this would result in the new clusters being in redox isolation from the other redox-active components of the mutant enzymes.

The substitution of Cys_{102} with Trp makes the sequence of Cys group III more homologous to that of the equivalent Cys group of the electron-transfer subunits (NarH and NarY) of *E. coli* nitrate reductases NarGHJI (Blasco et al., 1989) and NarZYWV (Blasco et al., 1990). The sequences of the Cys groups of the three enzymes are as follows:
It is likely that this Cys group of NarH provides ligands to the EPR- and MCD-detectable [3Fe–4S] cluster of purified nitrate reductase (Vincent, 1979; Johnson et al., 1985a), and on the basis of the sequence similarities between NarH and NarY, the latter probably also has a [3Fe–4S] cluster ligated by this Cys group. Thus, in addition to indicating the importance of the [4Fe–4S] cluster ligated by Cys group III of DmsB, our data also support the proposed role of NarH Cys group III in [3Fe–4S] cluster ligation suggested by Blasco et al. (1989). One of the possibilities raised by the mutagenesis reported herein is that one or more of the mutants may have altered reductase activity toward nitrate. We detected no significant alteration in substrate specificity of the mutants of DMSO reductase toward nitrate, although further studies are in progress to clarify this.

Construction of site-directed mutants of the conserved Cys residues in *E. coli* fumarate reductase has recently been reported by Werth et al. (1990). In this case, each of the four Cys residues thought to ligate the [2Fe–2S] cluster (FR1) was mutagenized to Ser residues. The resultant mutants of fumarate reductase retained cluster FR1, but the cluster had altered redox and EPR properties depending on which Cys residue was mutagenized. The $C_{102} \rightarrow S_{102}$ mutant of DmsB reported herein does not retain the [4Fe–4S] cluster ligated by the first three Cys residues of Cys group III in the wild-type enzyme, but has a [3Fe–4S] cluster ligated by these residues.

Martin et al. (1990) have recently reported site-directed mutagenesis of one of the Cys residues providing ligands to the [4Fe–4S] cluster of *Azotobacter vinelandii* ferredoxin I. Cys_{20} was changed to an Ala residue, and the mutant protein was able to retain the [4Fe–4S] cluster by using a redundant Cys elsewhere in the sequence (Cys_{24}) to replace Cys_{20}. Consequently, the structure of the mutant protein, as determined by X-ray crystallography, is perturbed relative to that of the wild-type protein. Although there are likely to be minor changes in the tertiary structure of DmsB resulting from the substitutions of Cys_{102} reported herein, these are not sufficient to prevent assembly of the DmsABC holoenzyme and its attachment to the cytoplasmic membrane.

Overall, the data reported herein show that it is possible to alter the [Fe–S] cluster composition of a complex respiratory chain enzyme by using oligonucleotide-directed mutagenesis. Further studies are in progress in this laboratory using the mutants of Cys_{102} and the equivalent Cys residues of the other Cys groups of DmsB with the aim of elucidating the role of each of the [4Fe–4S] clusters of wild-type DMSO reductase in electron transfer from menaquinol to DMSO.

ACKNOWLEDGMENTS

Thanks are due to Gillian Shaw for technical assistance, Ken Roy for oligonucleotide synthesis, Perry d'Obrenan and Rita Whitford for DNA sequencing, Richard Cammack for helpful discussions and advice on EPR spin quantitations, and Damaraju Sambasivarao for providing anti-DmsA and anti-DmsB immunoglobulins.

Registry No. DMSO reductase, 73200-91-6; Cys, 52-90-4.

REFERENCES

Beinert, H., & Thomson, A. J. (1983) *Arch. Biochem. Biophys. 222*, 333–361.
Bilous, P. T., & Weiner, J. H. (1985a) *J. Bacteriol. 162*, 1151–1155.
Bilous, P. T., & Weiner, J. H. (1985b) *J. Bacteriol. 163*, 369–375.
Bilous, P. T., & Weiner, J. H. (1988) *J. Bacteriol. 170*, 1511–1518.
Bilous, P. T., Cole, S. T., Anderson, W. F., & Weiner, J. H. (1988) *Mol. Microbiol. 2*, 785–795.
Blasco, F., Iobbi, C., Giordano, G., Chippaux, M., & Bonnefoy, V. (1989) *Mol. Gen. Genet. 218*, 249–256.
Blasco, F., Iobbi, C., Ratouchniak, J., Bonnefoy, V., & Chippaux, M. (1990) *Mol. Gen. Genet 222*, 104–111.
Bruschi, M., & Guerlesquin, F. (1988) *FEMS Microbiol. Rev. 54*, 155–176.
Cammack, R., & Weiner, J. H. (1990) *Biochemistry 29*, 8410–8416.
Cammack, R., Patil, D. S., & Weiner, J. H. (1986) *Biochim. Biophys. Acta 870*, 545–551.
Cole, S. T., Condon, C., Lemire, B. D., & Weiner, J. H. (1985) *Biochim. Biophys. Acta 811*, 381–403.
Condon, C., & Weiner, J. H. (1988) *Mol. Microbiol. 2*, 43–52.
Conover, R. C., Kowal, A. T., Fu, W., Park, J., Aono, S., Adams, M. W. W., & Johnson, M. K. (1990) *J. Biol. Chem. 265*, 8533–8541.
George, D. G., Hunt, L. T., Yeh, L. L., & Barker, W. C. (1985) *J. Mol. Evol. 22*, 20–31.
George, S. J., Armstrong, F. A., Hatchikian, E. C., & Thomson, A. J. (1989) *Biochem. J. 264*, 275–284.
Guigliarelli, B., Gyada, J. P., Bertrand, P., & More, C. (1986) *Biochim. Biophys. Acta 871*, 149–155.
Hagen, W. R., Dunham, W. R., Johnson, M. K., & Fee, J. A. (1985) *Biochim. Biophys. Acta 828*, 369–374.
Ingledew, W. J., & Poole, R. K. (1984) *Microbiol. Rev. 48*, 222–271.
Johnson, M. K., Bennett, D. E., Morningstar, J. E., Adams, M. W. W., & Mortenson, L. E. (1985a) *J. Biol. Chem. 260*, 5456–5463.
Johnson, M. K., Morningstar, J. E., Cecchini, G., & Ackrell, B. A. C. (1985b) *Biochem. Biophys. Res. Commun. 131*, 653–658.
Johnson, M. K., Kowal, A. T., Morningstar, J. E., Oliver, M. E., Whittaker, K., Gunsalus, R. P., Ackrell, B. A. C., & Cecchini, G. (1988) *J. Biol. Chem. 263*, 14732–14738.
Martin, A. E., Burgess, B. K., Stout, C. D., Cash, V. L., Dean, D. R., Jensen, G. M., & Stephens, P. J. (1990) *Proc. Natl. Acad. Sci. U.S.A. 87*, 598–602.
Mathews, R., Charlton, S., Sands, R. H., & Palmer, G. (1974) *J. Biol. Chem. 249*, 4326–4328.
Ohmori, D., Yamakura, F., Suzuki, K., Imai, T., & Nagayama, K. (1986) in *Iron–Sulfur Protein Research* (Matsubara, H., Ed.) pp 116–124, Springer-Verlag, Berlin.
Ohnishi, T., Ingledew, W. J., & Shiraishi, S. (1975) *Biochem.*

Biophys. Res. Commun. 63, 894-899.
Ohnishi, T., Blum, H., Sato, S., Nakazawa, K., Hon-nami, K., & Oshima, T. (1980) *J. Biol. Chem. 255*, 345-348.
Phillips, M. K., Hederstedt, L., Hasnain, S., Rutberg, L., & Guest, J. R. (1987) *J. Bacteriol. 169*, 864-873.
Prince, R. C., & Adams, M. W. W. (1987) *J. Biol. Chem. 262*, 5125-5128.
Rondeau, S. S., Hsu, P., & DeMoss, J. A. (1984) *J. Bacteriol. 159*, 159-166.
Rupp, H., Rao, K. K., Hall, D. O., & Cammack, R. (1978) *Biochim. Biophys. Acta 537*, 255-269.
Sambasivarao, D., Scraba, D. G., Trieber, C., & Weiner, J. H. (1990) *J. Bacteriol. 172*, 5938-5948.
Sambrook, J., Fritsch, E. F., & Maniatis, T. (1989) *Molecular Cloning: A Laboratory Manual*, 2nd ed., Cold Spring Harbor Laboratory Press, Cold Spring Harbor, NY.
Tartof, K. D., & Hobbs, C. A. (1987) *Bethesda Res. Lab. Focus 9*, 205.
Taylor, J. W., Ott, J., & Eckstein, F. (1985) *Nucleic Acids Res. 13*, 8765-8785.
Weiner, J. H., Cammack, R., Cole, S. T., Condon, C., Honore, N., Lemire, B. D., & Shaw, G. (1986) *Proc. Natl. Acad. Sci. U.S.A. 83*, 2056-2060.
Weiner, J. H., MacIsaac, D. P., Bishop, R. E., & Bilous, P. T. (1988) *J. Bacteriol. 170*, 1505-1510.
Werth, M. T., Cecchini, G., Manadori, A., Ackrell, B. A. C., Schroder, I., Gunsalus, R. P., & Johnson, M. K. (1990) *Proc. Natl. Acad. Sci. U.S.A. 87*, 8965-8969.
Westenberg, D. J., Gunsalus, R. P., Ackrell, B. A. C., & Cecchini, G. (1990) *J. Biol. Chem. 265*, 19560-19567.
Wilson, G. S. (1978) *Methods Enzymol. 54*, 396-410.
Vincent, S. P. (1989) *Biochem. J. 177*, 757-759.

Characteristics of the Combination of Inhibitory Mg^{2+} and Azide with the F_1 ATPase from Chloroplasts†

Marat B. Murataliev, Yakov M. Milgrom, and Paul D. Boyer*

The Molecular Biology Institute and the Department of Chemistry and Biochemistry, University of California, Los Angeles, Los Angeles, California 90024-1570

Received April 3, 1991; Revised Manuscript Received June 10, 1991

ABSTRACT: The interactions between ADP, Mg^{2+}, and azide that result in the inhibition of the chloroplast F_1 ATPase (CF_1) have been explored further. The binding of the inhibitory Mg^{2+} with low K_d is shown to occur only when tightly bound ADP is present at a catalytic site. Either the tightly bound ADP forms part of the Mg^{2+}-binding site or it induces conformational changes creating the high-affinity site for inhibitory Mg^{2+}. Kinetic studies show that CF_1 forms two catalytically inactive complexes with Mg^{2+}. The first complex results from Mg^{2+} binding with a K_d for Mg^{2+} dissociation of about 10–15 μM, followed by a slow conversion to a complex with a K_d of about 4 μM. The rate-limiting step of the CF_1 inactivation by Mg^{2+} is the initial Mg^{2+} binding. When medium Mg^{2+} is chelated with EDTA, the two complexes dissociate with half-times of about 1 and 7 min, respectively. Azide enhances the extent of Mg^{2+}-dependent inactivation by increasing the affinity of the enzyme for Mg^{2+} 3–4 times and prevents the reactivation of both complexes of CF_1 with ADP and Mg^{2+}. This results from decreasing the rate of Mg^{2+} release; neither the rate of Mg^{2+} binding to CF_1 nor the rate of isomerization of the first inactive complex to the more stable form is affected by azide. This suggests that the tight-binding site for the inhibitory azide requires prior binding of both ADP and Mg^{2+}.

One of the catalytic sites on the isolated F_1 ATPases from various sources binds ADP quite tightly (Futai et al., 1989; Harris, 1978; Strotmann, 1986). Such ADP together with Mg^{2+} participates in an unusual modulation of the catalytic activity (Carmeli et al., 1981; Drobinskaya et al., 1985; Feldman & Boyer, 1985; Milgrom & Boyer, 1990; Minkov et al., 1979, 1980; Zhou et al., 1988). When medium Mg^{2+} is present and ADP is bound at the catalytic site without bound P_i, a complex is formed that initially has little or no ATPase activity when Mg^{2+} and ATP are added (Drobinskaya et al., 1985; Feldman & Boyer, 1985; Milgrom & Boyer, 1990; Zhou et al., 1988). The ATPase activity can be restored by the chelation of medium Mg^{2+} with EDTA prior to assay of the enzyme with Mg^{2+} and ATP. If Mg^{2+} and ATP are added to the inactive complex, some ATPase activity slowly appears as the complex decomposes with release of the inhibitory ADP (Carmeli et al., 1981; Feldman & Boyer, 1985; Hackney, 1979; Vasilyeva et al., 1980, 1982).

Considerable uncertainty remains about the nature of the binding of the inhibitory Mg^{2+}. The apparent K_d for the binding to CF_1 is about 4 μM, and the inhibition may require the binding of only one Mg^{2+} per enzyme (Guerrero et al., 1990b). Where the inhibitory Mg^{2+} binds is not known. The CF_1 contains up to six binding sites for divalent Mn^{2+} or Mg^{2+} (Carmeli et al., 1979; Hiller & Carmeli, 1985, 1990), and three

† Supported by U.S. Public Health Service Grant GM-11094 and U.S. Department of Energy Grant P.A. FG03-88ER13845.

0006-2960/91/0430-8305$02.50/0